







Article

An Enhanced Innovative Triangular Trend Analysis of Rainfall Based on a Spectral Approach

Bilel Zerouali ^{1,*} , Nadhir Al-Ansari ^{2,*} , Mohamed Chettih ¹, Mesbah Mohamed ³, Zaki Abda ¹ , Celso Augusto Guimarães Santos ⁴ , Bilal Zerouali ⁵  and Ahmed Elbeltagi ^{6,7} 

- ¹ Research Laboratory of Water Resources, Soil and Environment, Department of Civil Engineering, Faculty of Civil Engineering and Architecture, Amar Telidji University, Laghouat 3000, Algeria; m.chettih@lagh-univ.dz (M.C.); z.abda@lagh-univ.dz (Z.A.)
- ² Department of Civil, Environmental and Natural Resources Engineering, Lulea University of Technology, 97187 Lulea, Sweden
- ³ Earth Sciences Faculty, University of Science and Technology Houari Boumediene, BP 32, Bab Ezzouar 16311, Algeria; mohamed_mesbah@hotmail.com
- ⁴ Center for Technology, Department of Civil and Environmental Engineering, Federal University of Paraíba, João Pessoa 58051-900, Paraíba, Brazil; celso@ct.ufpb.br
- ⁵ Petrochemical and Process Engineering Department, 20 August 1955 University, 26 Road, El Hadaiek-Skikda 21000, Algeria; zeroualibilal3@gmail.com
- ⁶ Agricultural Engineering Department, Faculty of Agriculture, Mansoura University, Mansoura 35516, Egypt; ahmedelbeltagi81@mans.edu.eg
- ⁷ College of Environmental and Resource Sciences, Zhejiang University, Hangzhou 310058, China
- * Correspondence: b.zerouali@lagh-univ.dz (B.Z.); nadhir.alansari@ltu.se (N.A.-A.)



Citation: Zerouali, B.; Al-Ansari, N.; Chettih, M.; Mohamed, M.; Abda, Z.; Santos, C.A.G.; Zerouali, B.; Elbeltagi, A. An Enhanced Innovative Triangular Trend Analysis of Rainfall Based on a Spectral Approach. *Water* **2021**, *13*, 727. <https://doi.org/10.3390/w13050727>

Academic Editor: Chunhui Li

Received: 17 January 2021

Accepted: 2 March 2021

Published: 7 March 2021

Publisher's Note: MDPI stays neutral with regard to jurisdictional claims in published maps and institutional affiliations.

Abstract: The world is currently witnessing high rainfall variability at the spatiotemporal level. In this paper, data from three representative rain gauges in northern Algeria, from 1920 to 2011, at an annual scale, were used to assess a relatively new hybrid method, which combines the innovative triangular trend analysis (ITTA) with the orthogonal discrete wavelet transform (DWT) for partial trend identification. The analysis revealed that the period from 1950 to 1975 transported the wettest periods, followed by a long-term dry period beginning in 1973. The analysis also revealed a rainfall increase during the latter decade. The combined method (ITTA–DWT) showed a good efficiency for extreme rainfall event detection. In addition, the analysis indicated the inter- to multiannual phenomena that explained the short to medium processes that dominated the high rainfall variability, masking the partial trend components existing in the rainfall time series and making the identification of such trends a challenging task. The results indicate that the approaches—combining ITTA and selected input combination models resulting from the DWT—are auspicious compared to those found using the original rainfall observations. This analysis revealed that the ITTA–DWT method outperformed the ITTA method for partial trend identification, which proved DWT's efficiency as a coupling method.

Keywords: innovative triangular trend analysis; discrete wavelet transform; hybrid method; rainfall; Algeria



Copyright: © 2021 by the authors. Licensee MDPI, Basel, Switzerland. This article is an open access article distributed under the terms and conditions of the Creative Commons Attribution (CC BY) license (<https://creativecommons.org/licenses/by/4.0/>).

1. Introduction

Since the beginning of the 1900s, the spatiotemporal variability of precipitation caused by climate change has been a significant concern for water resource managers around the world [1–7]. It was found that such variability directly affects the effectiveness of the water resource system, which sometimes leads to imbalances in an even precipitation distribution, especially for the development in some fields, such as agriculture, industry, and civil engineering [8].

Establishing sensitive and effective management systems is not sufficient by itself for managing water resources. It instead requires reasonable and accurate control of

the water cycle components, especially precipitation and temperature. Thus, developed countries strive to develop tools and devices to monitor and measure these components [9]. The success of this system is not complete without the availability of analysis tools and competent persons. In Algeria, for example, despite the many kinds of research that have been done in the field of geosciences, hydrology, and water resources [10–17], it is insufficient to assess climatic conditions and their impact on the environment [18], and to find accurate future solutions to manage crises and natural disasters, such as long-term droughts, floods, and management of hydraulic structures [19]. This is due to its vast area, abundant natural resources, climate, environmental diversity, and unsatisfactory conditions to support research.

For example, in the hydrology field of flood prediction, management engineers sometimes face problems in the calibration and validation of rainfall–runoff models to better manage hydraulic infrastructures [14]. The existence of hidden characteristics, in terms of multiple change points, trends seasonality, stationarity, and extreme events in the time series to be used in the modeling process, constitutes one of the problems that affect the calibration and validation of such models [20]. It is worth noting that those characteristics also make the rainfall–runoff relationship more nonlinear. Moreover, according to [14,21], in case of the lack of statistically significant patterns in the long-term (upward/downward) in a rainfall time series, except for shorter periods, the inter-annual to inter-decadal modes of variability can give a contribution to hiding long-term patterns in the time series. Although mathematical and statistical methods facilitate the detection of these properties, they sometimes seem to have limited efficiency. Such anomalies may appear in the rainfall time series, but not in the stream flow time series, because the latter can suffer human interference. For example, [22] found that, in the Sebaou River basin (northern central of Algeria), the rainfall and discharge relationship was nonlinear, which could be mainly due to the drought events. Moreover, the analysis, research, and investigation of the field revealed that the Taksebt dam's commissioning and the smuggling and trafficking of rocks and sands from the riverbed since 1998 has had a negative and significant influence on the river flow amount. In the Ramganga River basin (India), as noted by [23], climate change and anthropogenic activities were the main factors affecting the significant decline in water basin storages between 1982 and 2013.

The 1960s marked the beginning of the computer revolution, which led to a quantum leap in hydrological modeling development [24]. Several hydrology researchers across the world have developed mathematical and statistical methods that have been used in hundreds of research papers, due to their success in determining changes in time series', such as parametric and non-parametric tests. The latter is the most used in research studies, such as the Mann–Kendall test, Pettitt's test, and Sen's slope estimator test [25–34], among others. Parametric tests are generally excellent, yet they require the data to follow the assumed distribution law effectively. They are mainly very sensitive to outliers and are not recommended if outliers are detected. Non-parametric tests do not need to assume a particular type of distribution to calculate the test's alpha risk. They are based on numerical properties, and they are very insensitive to outliers, and are therefore recommended in this case [31]. In 1980, the up-and-coming trend involved the use of the wavelet theory, in the earth science time series analysis as geology [35], geophysics [36], hydrology [37], and climatology [14,38]. The wavelet theory can detect invisible abnormalities and change points in time series compared to other analyses. The application of wavelet theory brought about a great revolution in analyzing non-stationary phenomena, especially for the most extended observations. In recent years, the use of artificial intelligence tools, such as neural networks and deep learning, for example, have been fiercely competing with all methods of analyzing and predicting rainfall and detecting alerts of droughts and wet years [39,40].

One recent method that proposed for hydroclimatic variability assessment is the innovative trend analysis (ITA), which was first elaborated by [41]. The methodology is known for its effectiveness and success for partial trend component identification. It was used in hundreds of research studies, primarily in the earth science field [20,42–51].

The success of innovative trend methodology [38] made it a method of interest to many scientists and researchers worldwide. That is why they continued conducting scientific experiments and technical contributions on this method, to improve its performance, mainly for temporal trend detection, primarily in a complicated hydro-climatic time series. For example, a combination of Sen's trend method with the discrete wavelet transformation (DWT) was applied by [52], who were among the first rank to implement the proposed hybrid model. Their findings stated the effectiveness of this adapted method. However, a statistical significance test application has been added to ITA [41] by [53,54], to improve its reliability using a synthetically generated time series that included deterministic, ordinary, and stochastic processes, and gamma stochastic process tests. The paper revealed that all of the steps of the methodology were logically presented and easy to apply. In [55], the authors proposed a significance level of 5 and 10% for trend magnitude interpretation. In [44], the authors elaborated two methods inspired by ITA, known as the double- and triple- of the ITA. These two methods are referred to as multiple Sen-innovative trend analyses, where the time series' were split into three subsections for Double-ITM (D-ITA) and four sub-series for Triple (T-ITA) before introducing them into the Sen's template calculator. The comparison of the sub-series' indicates acceptable identification of trend stability. An improved version of ITA was proposed by [56], based on an approach of the change boxes. Outcomes indicated that the new hybridization method had efficaciously enhanced the numerical illustration of time series changes on ITA's scatter graph. At this time, all critical points for Sen's trend analysis presented in the literature are successfully discussed by [57]. The latest inspired method based on ITA is called the innovative triangular trend analysis methodology (ITTA), which was proposed by [58]. ITTA is based on dividing the time series into subintervals (series) of equal length and comparing each, pairwise, in the form of a triangular array [58]. In [14], the authors assessed four comparatively recent hybrid approaches for change points and trends detection; the first is called the dynamic programming Bayesian change point method (BA) [56], the second is the innovative trend analysis [41], while the third and the fourth are double and triple of the ITA, respectively, in conjunction with DWT, based on a multi-resolution analysis.

According to our knowledge in hydrology and climatology science, particularly in change point and trends detection in hydroclimatic time series, the most recent research has not devoted much value to addressing noise quantization and the respective impact on the results. Modern research in hydrology has begun with interest in assessing and reducing noise in hydrological time series' using time–frequency methods, especially in the past ten years, when the most research has focused on using DWT with non-parametric statistical tests [29,38]. In ITA's framework [41], and the inspired methods, the author developed another hybrid approach, where the first method “innovative triangular trend analysis methodology” was embedded with wavelet transforms (ITTA–DWT). The DWT was used as a noise reduction and preprocessing tool for improving the effectiveness of ITTA for partial trend identification. The proposed hybrid method was assessed on data from three representative stations in northern Algeria, from 1920 to 2011, on an annual scale.

2. Materials and Methods

The flowchart represented in Figure 1 was proposed for the preprocessing and analysis of the selected rainfall time series by combining the innovative triangular trend analysis (ITTA) (Table 1) with the orthogonal discrete wavelet transform (DWT), i.e., a hybrid method (ITTA–DWT), which can be addressed in the following steps:

1. Pretreatment of the input rainfall signal $X(t)$.
2. Using filter bank includes high pass filter (A) and low pass filter (D) for signal filtering.
3. The outputs of A and D are downsampled by the DWT scale coefficient (factor of 2).
4. Choosing the adequate sub-band signal or the scale of decomposition for downsampling based on the time series length.
5. Selecting the mother- and daughter-wavelet, e.g., Daubechies mother-wavelet (db20).
6. After step 5, the wavelet coefficients are obtained.

7. From the wavelet coefficients (approximations and details), 24 models were proposed (Table 2), assessed, and analyzed using correlation and spectral analyses for assessing the periodicity and to perform the filtering
8. The 24 proposed models were used as input time series into the ITTA.

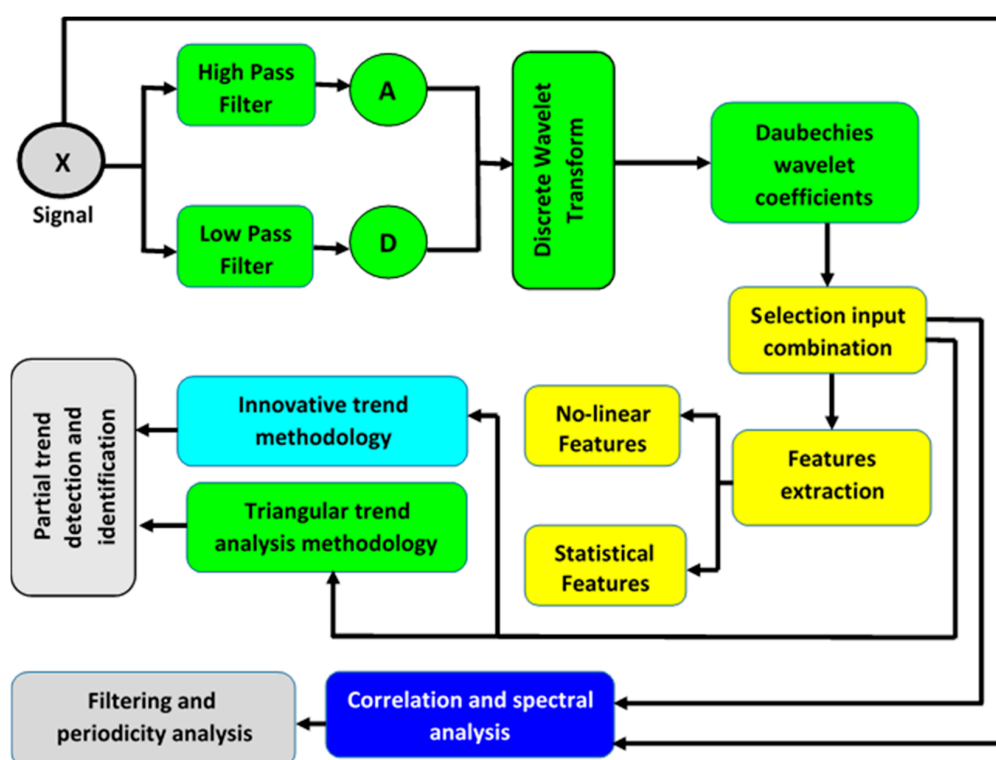


Figure 1. Flowchart proposed for the analysis combining innovative triangular trend analysis (ITTA) with discrete wavelet transform (DWT) (ITTA–DWT: hybrid method).

Table 1. Theoretical ITTA comparison set proposed by [58].

Sub-Series	1st	2nd	3rd	4th	(n/t)th
1st	1	1st–2nd	1st–3rd	1st–4th . . .	1th–(n/t)th
2nd		1	2nd–3rd	2nd–4th . . .	2nd–(n/t)th
3rd	Meaningless		1	3rd–4th . . .	3rd–(n/t)th
4th				1	4th–(n/t)th
(n/t)th					1

2.1. Triangular Trend Analysis Methodology

As ITA inspires the ITTA method, [58] used the ITA template proposed and explained by [41] to build the ITTA, which was verified through several simulations [53,54].

It is dependent on comparing between the two equal observation intervals. The interval-I and the period-II are respectively placed on the horizontal x-axis and the vertical y-axis and ordered in an ascendant manner. In the case of trendless time series (no trend), the observation points will appear high correlated to the 1:1 (45°) straight line. In decreasing or increasing trend, data points will be placed below or above the trendless line, respectively (Figure 2). Each tendency is classified and interpreted according to the three quantities (small, moderate, and high), according to Figure 2. As mentioned earlier, the ITTA is based on dividing the time series into sub-intervals and comparing each, pairwise, in the triangular array form (Table 1), as proposed by [58]. For more clarifications, the reader is invited to consult the research paper of [58–60].

Table 2. Geographic, statistical, and nonlinear characteristics of the rainfall series and their 24 proposed models resulting from the discrete wavelet analysis.

Oued Taria Station X = 274.4 km Y = 176.4 km Z = 1000 m						Azazga Station X = 649.6 km Y = 383.9 km Z = 430 m				Ain Beida Station X = 924.15 km Y = 288 km Z = 1004 m			
Model (M)	Combination	R ₁ ²	Min	Max	CTV (%)	R ₂ ²	Min	Max	CTV (%)	R ₃ ²	Min	Max	CTV (%)
OS	-	1.00	72	754	100	1.00	521	1577	100	1.00	155	631	100
M 1	D1	0.30	−169	195	30.6	0.43	−398	360	43.1	0.42	−154	152	41.4
M 2	D2	0.22	−124	139	20.7	0.28	−364	288	29.8	0.32	−94	89	30.3
M 3	D3	0.05	−51	55	5.6	0.07	−149	165	11.2	0.06	−61	64	7.0
M 4	D4	0.09	−68	66	9.5	0.06	−118	126	6.3	0.09	−64	40	10.6
M 5	D5	0.08	−68	82	13.7	0.10	−113	134	11.0	0.05	−16	10	0.8
M 6	A5	0.20	278	423	24.5	0.01	945	1036	1.2	0.09	350	437	7.6
M 7	D1+A5	0.50	179	618	54.9	0.44	585	1363	44.4	0.51	242	546	49.2
M 8	D2+A5	0.40	174	561	45.5	0.29	642	1291	31.1	0.40	256	494	38.1
M 9	D3+A5	0.25	228	451	30.4	0.09	799	1110	12.1	0.16	332	461	14.0
M10	D4+A5	0.29	220	445	34.2	0.07	849	1092	7.7	0.19	287	465	17.3
M 11	D5+A5	0.33	213	417	32.9	0.12	835	1104	12.4	0.10	339	443	11.4
M 12	D1+D2+A5	0.71	140	732	76.1	0.72	591	1650	74.3	0.81	223	617	80.0
M 13	D1+D2+D3+A5	0.76	100	753	81.9	0.82	530	1602	82.9	0.88	210	616	87.0
M 14	D1+D2+D3+D4+A5	0.86	54	769	91.7	0.88	530	1627	89.0	0.99	163	625	96.3
M 15	D1+D2+D3+D5+A5	0.90	119	738	90.2	0.93	519	1594	93.9	0.89	198	622	90.7
M 16	D1+D3+D4+D5+A5	0.79	149	640	78.9	0.70	482	1434	71.9	0.69	194	560	68.9
M 17	D1+D3+D4+A5	0.65	130	655	70.6	0.61	512	1480	62.2	0.68	187	554	65.1
M 18	D1+D4+D5+A5	0.74	175	619	73.1	0.71	512	1480	62.2	0.62	227	561	62.7
M 19	D2+D4+D5+A5	0.63	80	571	63.7	0.45	644	1374	49.3	0.51	190	525	51.4
M 20	D3+D4+D5+A5	0.48	178	472	48.3	0.27	729	1253	28.6	0.27	276	480	27.2
M 21	D4+D5+A5	0.43	192	451	42.6	0.18	826	1226	18.9	0.20	276	469	21.1
M 22	D3+D5+A5	0.39	187	432	38.7	0.20	686	1165	22.7	0.17	337	471	17.8
M 23	D2+D5+A5	0.54	132	549	53.9	0.20	605	1328	42.6	0.41	248	500	41.8
M 24	D1+D5+A5	0.64	158	603	63.3	0.55	558	1356	55.6	0.51	226	551	53.0

CTV: Contribution in total variance, D: detail of X_i and A: approximation of X_i .

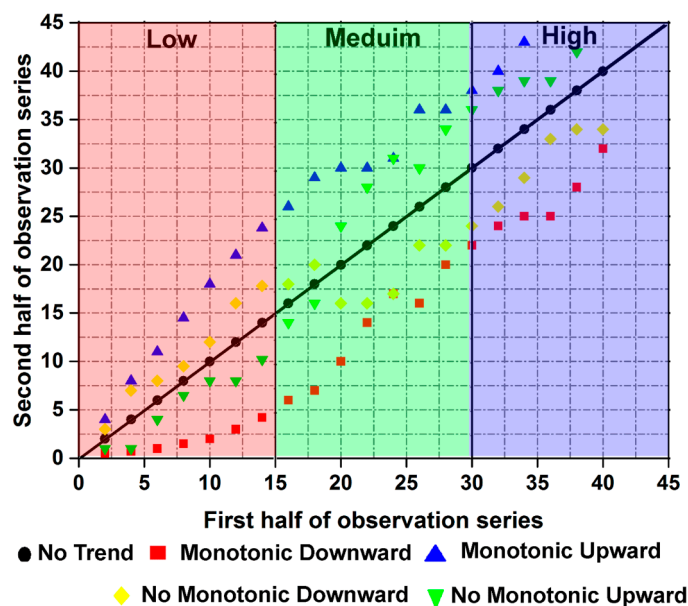


Figure 2. Innovative trend methodology template (the black dots are data with no trends) [41].

In this study, one scenario of an 18-year sub-time interval was chosen based on the following purposes:

- To exploit the entire available time series.
- To always stay within the original methodology (same template) and for comparative purposes.
- To extract and detect long-term and significant partial trends.

However, in the future, different sub-time intervals can be used for detecting new atmospheric fluctuations, which would help with understanding the climate variability within Algeria for better water resource planning.

2.2. Discrete Wavelet Transform

The discrete wavelet transform (DWT) algorithm was first introduced and proposed in 1989 by Stéphane Mallat [60]. It can be used in denoising, filtering, compressing, and decomposing the signal and its variance by dissociating its components at various scales. It also offers an excellent analysis of the signals and facilitates detection of the non-stationarity in the signal, where this feature is not available in classic techniques, such as short-time Fourier transform (STFT) and Fourier transform (FT). The main equations of DWT of the time series is:

$$W_{m,n} = 2^{-m/2} \sum_{i=0}^{N-1} x_i \psi(2^{-m} i - n) \quad (1)$$

where $W_{m,n}$ is the DWT coefficient of scale $s = 2^m$ and position $\tau = 2^m n$. Mallat 1989 defines the DWT as follow:

$$x(i) = A_x^m(i) + \sum_{j>m+1} D_x^j(i) = A_x^m(i) + R_x^j(i) \quad (2)$$

A^m : The approximation of the discrete signal $x(i)$ at the resolution m . D^m : the detail of the discrete signal of $x(i)$ at the resolution m . R_x^m : the residue at the approximation scale m . DWT informs change in an input chronological series at various scales and positions. The papers of [57–59] explain well the implantation of DWT.

2.3. Correlation and Spectral Analysis

The simple correlation analysis highlights the dependence of successive events for increasing time intervals [60–64]; it based on the autocorrelation function for a time series of N observations $x_t(x_1, x_2, x_3, \dots, x_n)$ and \bar{x} mean [65].

The values r_k ($k = 0, 1, 2, \dots, m$) are the autocorrelation coefficients obtained. According to Box and Jenkins 1976; the choice of truncation (m) is not based on theoretical concepts, it is better to take $m = N/2$, $m = N/3$ or $m = 2N/3$. The following expression gives r_k :

$$r_k = \frac{C_k(k)}{C_k(0)} \quad (3)$$

With

$$C_k(0) = \frac{1}{N} \sum_{t=1}^N (x_t - \bar{x})^2 \quad C_k(k) = \frac{1}{N} \sum_{t=1}^{N-k} (x_t - \bar{x}) (x_{t+k} - \bar{x}) \quad (4)$$

$C_k(k)$: is the auto covariance and k : is the time step.

According to [66]: power spectral density function $\Gamma_x(f)$ is an unbiased approach of the Fourier transform of the function of autocorrelation, representing the decomposition of the time series variation in the hesitation area, where the periodic phenomena show up as peaks in $\Gamma_x(f)$ graph [63,64] is provided by:

$$\Gamma_x(f) = 2 \left[1 + 2 \sum_{k=1}^m D_k r_k \cos(2\pi f k) \right] \quad (5)$$

f : is the frequency, D_k is a weighting function chosen in such a way that has the estimated value of the spectrum $\Gamma_x(f)$ is not biased [66]. The Tukey filter is used, and in this case:

$$D_k = \frac{1 + \cos\left(\frac{\pi k}{m}\right)}{2} \quad (6)$$

2.4. Study Area and Collected Data

In this proposed work, annual data of rainfall from 1920 to 2011 were derived from the three extreme representative stations, which are situated in the north and north side of Algeria, and used for the scale analysis (Figure 3 and Table 2). The Mediterranean climate is characterized by warm to hot, dry summers, and mild to cool, wet winters. It is also characterized by a high diversity of climate trends relating to relief, watershed orientation, and the distance from the sea. The climate of Algeria is dependent on the air mass movement (North Atlantic) cold and wet (responsible for low temperatures and heavy rains) tropical ocean; warm humid, associated with the Azores anticyclone [10,12,15–19]. Therefore, the climate of Algeria is varied, since the country has a very large area. The northern part has a Mediterranean climate, while the rest of the country mainly has a desert climate (Köppen classification) [18]. Thus, three rainfall stations were proposed for the analysis to try to get a glimpse regarding climate variability of northern Algeria. In addition, this selected geographical region has a limited research focus.

Oued Taria station is located southwest of the Macta watershed (Figure 3). It is located between west longitude $1^\circ 16'$ and $0^\circ 58'$ and north latitude $34^\circ 31'$ and $35^\circ 21'$. This basin is considered one of the biggest Mediterranean basins in northwestern Algeria, occupying an area of $14,389 \text{ km}^2$. A Mediterranean climate dominates the northern part of the Macta. However, the southern interior part is characterized by a hot and dry climate in summer, and cold and humid in the winter (Figure 3). The Azazga station is located in the Oued Sebaou watershed (Figure 3), which extends to the extreme northern–central section of Algeria, between north latitudes $36^\circ 30'$ and $37^\circ 00'$ and east longitudes $3^\circ 30'$ and $4^\circ 30'$. This basin is one of the most watered basins in the Mediterranean, and it covers an area of 2500 km^2 (Figure 3). The Ain Beida station is located in the endorheic basins of the

Constantine highlands (Figure 3), representing the semiarid areas of northeastern Algeria, and covers an area of 9615 km² (Figure 3).

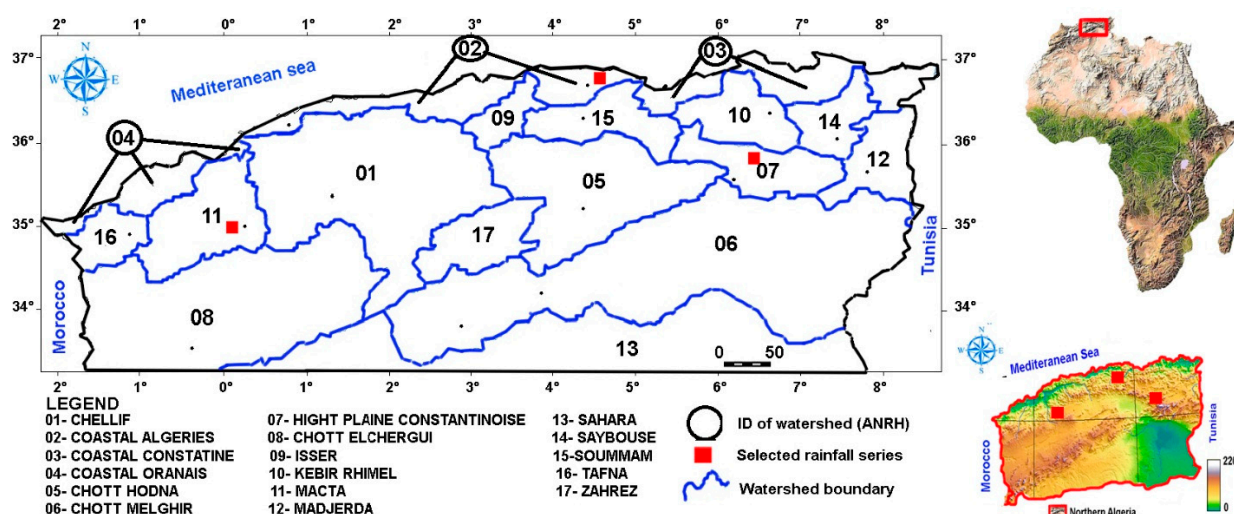


Figure 3. Northern Algeria and selected rainfall series used in the analysis.

3. Results and Discussion

3.1. Triangular Trend Analysis Methodology

For innovative triangular trend analysis methodology, the rainfall time series of 92 years were divided into five successive periods of eighteen years (1920–1937, 1938–1955, 1956–1973, 1974–1991, and 1992–2009) before inserting on Şen's graph template. In the first observation, by comparing ITA (the bottom left corner) with ITTA (top right corner), the visual observation demonstrates that the ITTA provides more information and details regarding partial trend components than ITA. This is one of the advantages of ITTA. For the Oued Taria rainfall, the ITA indicates a significant monotonic downward rainfall trend where the negative part of the trend was observed in 1966–2011 for low, medium, and high magnitudes (Figure 4). The first row of ITTA indicates no monotonic downward trend for the 1938–1955, 1956–1973 periods and a monotonic downward trend for the 1974–1991 and 1992–2009 compared to 1920–1937 (Figure 4). The second row revealed no monotonic upward rainfall trend for 1956–1973 compared to 1938–1955 with points appearing highly correlated to the 1:1 (45°) straight line, characterizing a downward trend for the 1974–1991 and 1992–2009 periods, compared to 1938–1955. For the third row, a monotonic downward trend is observed for the 1974–1991 and 1992–2009 periods compared to 1956–1973. The fourth-row analysis revealed that the 1992–2009 period carried part of the trend (no monotonic) than the 1974–1991 period (Figure 4).

Likewise, in several Tunisia regions, many authors declared the absence of significant annual trends, or that these trends are not always detected [66–72]. According to [14,21], the lack of statistically relevant long-term rainfall patterns, except for shorter periods, can be attributed to the inter-annual of the inter-decadal mode of variability, which will help to mask long-term patterns in a rainfall period series.

Furthermore, the western Mediterranean basin is located in the transition between mid-latitudes and a tropical zone, in which atmospheric dynamic interacts with a complex topography to produce a high spatiotemporal variability of rainfall [73]. Based on the coefficient of variation (CV) and the consecutive disparity index (S), [74] showed the strongest influence of the Western Mediterranean Oscillation (WeMO) over locations in which precipitation irregularity was highest (high CV and S values), and vice versa. According to [75], rainfall trends over southern Tunisia may be influenced by the rainfall regime (local changes) rather than large-scale climatic fluctuations.

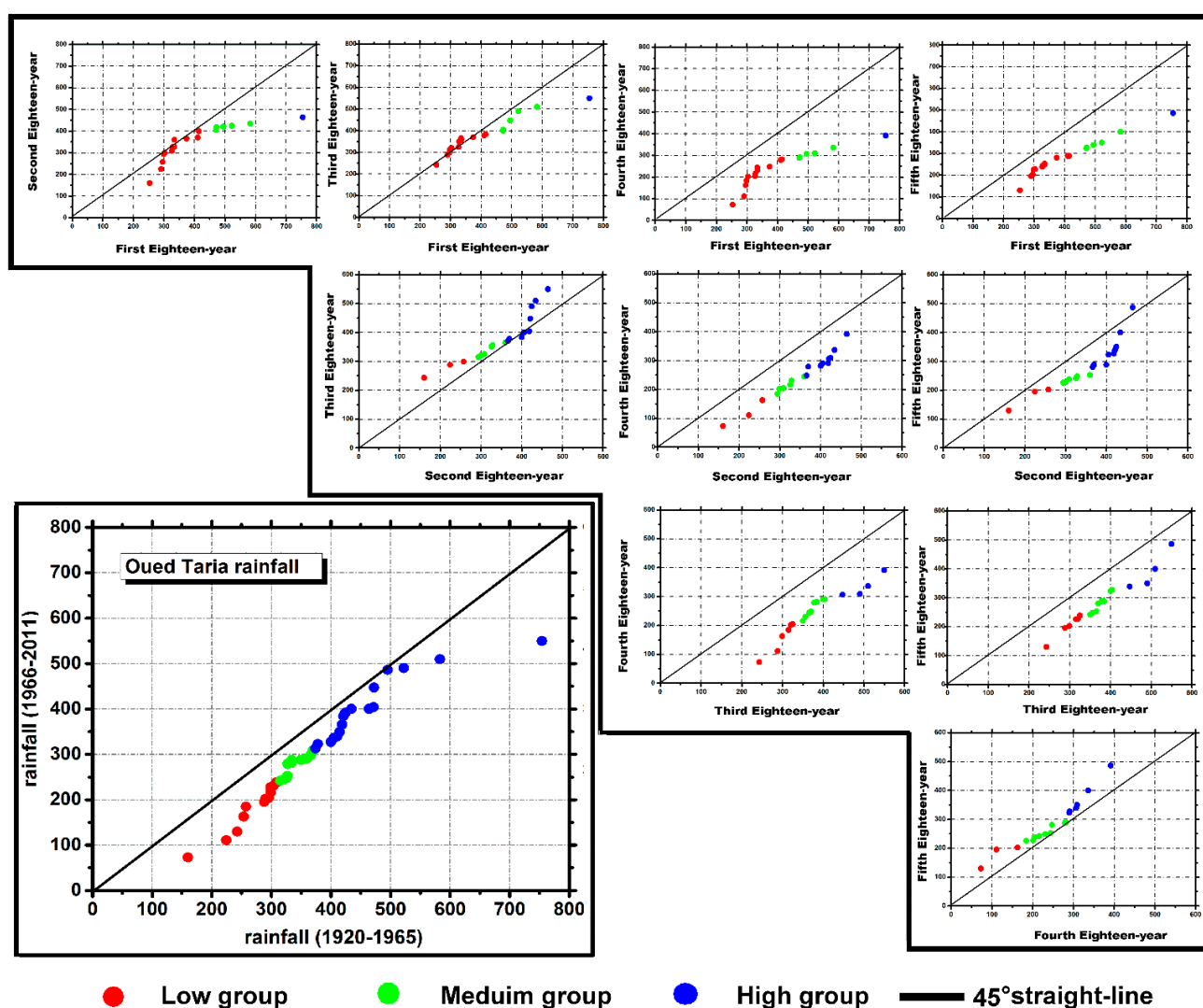


Figure 4. Triangular trend analysis methodology applied on rainfall series of Oued Taria.

The analysis of Azazga and Ain Beida rainfalls using ITA and ITTA (Figures 5 and 6) indicated that observation points appear very close to the 1:1 (45°) straight line, making the decision about the existence of significant partial trend components for different rainfall magnitude very difficult. According to many research pieces, western Algeria (Macta basin, for example) is recommended for climate change assessment and its impact studies [67]. Western Algeria is more vulnerable to drought impact, and this is explained by the fact that the Rif Mountain Range and the High Atlas Range (Morocco) are acting as barriers to prevent the incoming moist air from arriving from the Atlantic Ocean. Besides, winds, which are in northwestern side, recharge on the Mediterranean Sea to produce strong amounts of rainfall on the northern side, and superimpose a rainfall increase with longitude (from the west to the east). This is a particular characteristic in Algeria, which makes the Sebaou River basin one of the most watered in northern Algeria compared to the Macta basin (western Algeria). Many authors revealed that the Mediterranean climate impacts the high rainfall variability in northern Africa and southern Europe. For example, based on long-term rainfall series analysis, [68] observed that the Mediterranean area's rainfall variability has become irregular over time, with drier and extreme climatic conditions. In [21,69], the authors revealed the lack of a statistically significant long-term trend in rainfall in the Mediterranean basin resulting from the strong heterogeneity of the regional scale.

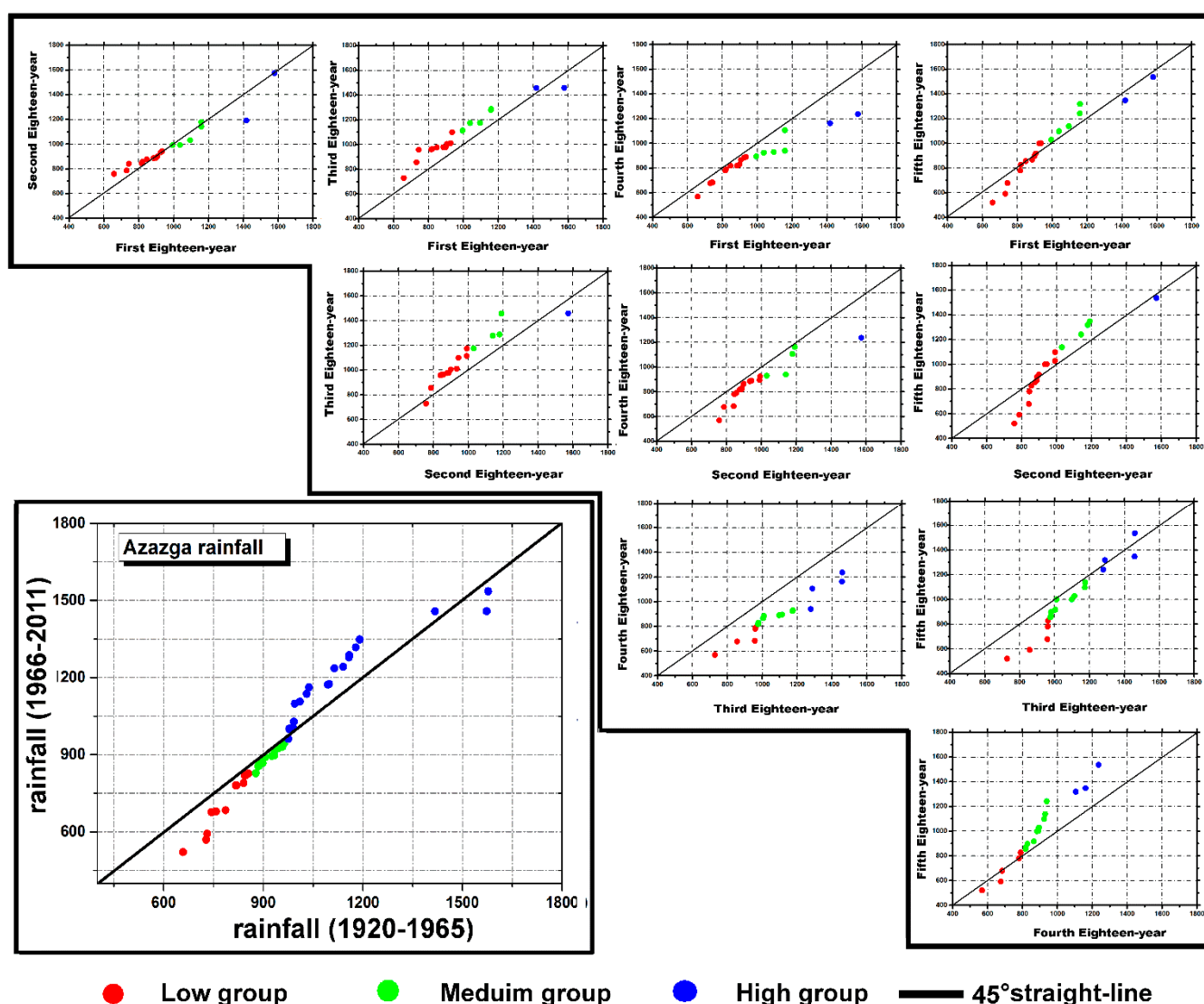


Figure 5. Triangular trend analysis methodology applied on rainfall series of Azazga.

According to the scientific community in hydrology, climatology, and meteorology, the high rainfall variability can be attributed to geographic factors (as latitude, longitude, and elevation), distance from the sea and large bodies of water, position to mid-latitudes and tropical, topography, vegetation, prevailing winds and ocean currents provoking large scale climatic phenomena responsible for multiannual and multi-decadal fluctuations, in addition to the errors of measuring devices, which may increase the noises. The authors are well aware that most of these factors can influence one time on a particular area's rainfall. All of these factors can influence the time series of rainfall measurements' physical values, which contribute to producing or adding the noise component in the original signal, making it difficult for diagnosis and analysis. Therefore, the tool used in the analysis may not necessarily be of limited effectiveness. However, instead, it is necessary to study the fluctuations of the time series with specific tools and methods, before starting the analysis process with change points and trend detection methods. This is for better interpretation of results and decision-making. For example, using quantitative rainfall analysis-based ITA in the Macta watershed, [51] noticed that "low and medium" rainfall ranges commonly have no-trend cases, but "high" rainfall values have decreasing trends, likewise, [14] using ITA, observed a non-significant upward trend in Oued Taria and no rainfall trend in Azazga and Ain Beida stations. Nevertheless, with the time-frequency-based method as a preprocessing and combined approach (ITA-DWT), [14] successfully detected hidden

change points in the rainfall time series. For this, in this paper, in addition to three rainfall series, 24 input combinations for each rainfall station resulting from DWT were assessed using ITTA to partial trend identification.

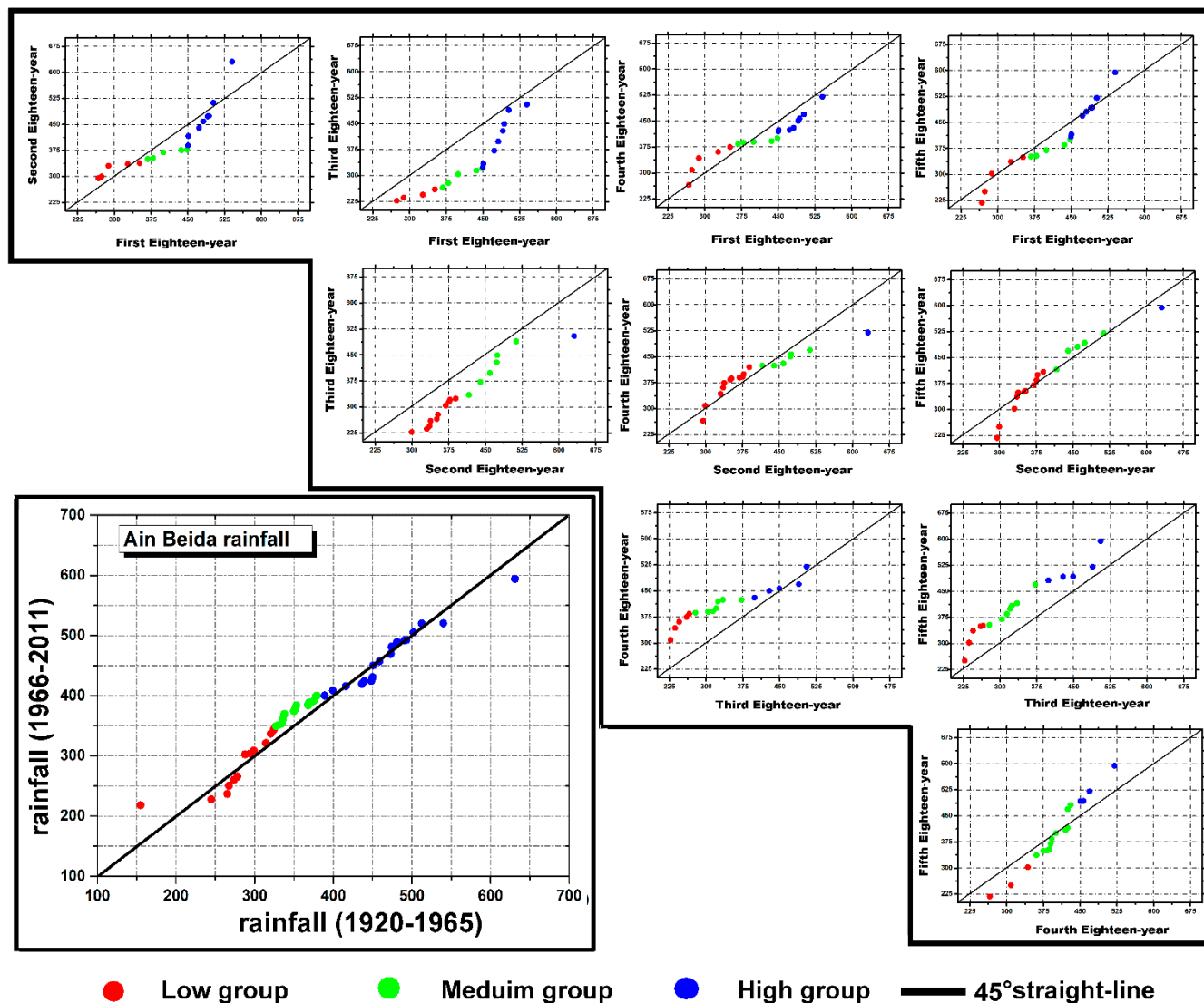


Figure 6. Triangular trend analysis methodology applied on rainfall series of Ain Beida.

3.2. Combining Triangular Trend Analysis Methodology with Discrete Wavelet Transform

The first row of ITTA indicates no monotonic downward trend for the 1938–1955, 1956–1973 periods, and a monotonic downward trend for the 1974–1991 and 1992–2009 compared to 1920–1937 (Figure 4). The second row revealed no monotonic upward rainfall trend for 1956–1973 compared to 1938–1955, with points appearing highly correlated to the 1:1 (45°) straight line, characterizing a downward trend for the 1974–1991 and 1992–2009 periods, compared to 1938–1955. For the third row, a monotonic downward trend is observed for the 1974–1991 and 1992–2009 periods compared to 1956–1973. The fourth-row analysis revealed that the 1992–2009 period carried part of the trend (no monotonic) than the 1974–1991 period (Figure 4). Noise is a series of small explosions in the signal. It is an unwanted signal that contaminated the measurement of another series. Its power spectrum, average, and variance are non-stationary over time. It is a time series that contains information about the origin of the noise. A variety of sources causes such noises. Distortion and noise effect reduction in the signal has become the core of the

signal processing and communication theory and application, such as medical image processing, radar, speech recognition [76], and others. One of the most known noise reduction approaches is low-pass filtering, based on a threshold selection of the power spectrum. The second stage removes all components whose frequency is greater than the threshold selected [77]. Signal-to-noise ratio (SNR) and linear approaches, such as Fourier transformation, are also used [78], but the latter is not recommended.

As stated earlier, the recent researches started around ten years ago to consider signal noise quantization and reduction in hydrological time series' using time–frequency based methods, such as [79], who designed a new approach using continuous wavelet transform coefficients for trend detection, which was considered one of the preferred combined approaches, especially for complicated time series. The success of the hybrid methods has a great revolution in the field of hydrology, where many researchers have suggested and proposed many hybrid approaches [7,14,29,52,80–84]. Nevertheless, most research has focused on using DWT with non-parametric statistical tests. Quite the opposite when predicting the future hydroclimatic parameters, researchers have been creative in using time–frequency-based approaches with various types of artificial intelligence algorithms, such as neural network, neuro–fuzzy approach, and extreme learning machine [85–87], but this application is still in its beginning stage, which opens the way for more development in the future.

Many researchers and authors suggested similar combinations as presented in Table 2 [7,52,80,83,88–90]. These proposed models may not have a central role to play in the decision-making process regarding trend component existence [14,81].

The 24 proposed models resulting from DWT of Table 2 are well represented and explained in [14]. The DWT approximations (A) and details (D) at five levels are represented hereafter as A1, A2 ... A5 and D1, D2 ... D5, respectively. More details about the implementation of DWT can be found in References [5,60–62]. The nonlinear fluctuations and climatic responses of each spectrum (Model) were interpreted in the framework of climate variability [14]. The results of [14] indicate that the hybridization models of the BA–DWT, ITA–DWT, D–ITA–DWT, and T–ITA–DWT, in most cases, generate high performance compared to the traditional approach (BA, ITA, D–ITA, and T–ITA). Furthermore, the results revealed that removing some spectrums of the original series using DWT significantly improved the accuracy of detecting hidden patterns and shift points. Therefore, in this section, we will attempt to confirm or disagree with the hypothesis proving DWT's efficiency as a coupling method that can improve ITTA accuracy for partial trend component identification.

In this section, a relatively new hybrid method, ITTA–DWT, was presented to enhance the temporary localization and facilitate the numerical or graphical visualization of the partial trends on the ITTA dispersion graph based on Şen's template. The best hybrid models, ITTA–DWT, are shown in Figures 7–9.

The analysis indicates that model 20, containing the sum of D3, D5, and A5, characterizes a significant partial trend in the station of Oued Taria. The graphical representation revealed a significant negative monotonic trend, particularly for low and medium rainfall for the periods: 1938–1955, 1956–1973, 1974–1991, and 1992–2009 compared to the period 1920–1937. The second row revealed an increased partial trend for the third 18-year period, 1956–1973, compared to the second, 1938–1955, marked for low and medium rainfall. In contrast, the fourth and fifth 18-year period revealed a tendency towards drier conditions than the second period. The last row of ITTA indicates an increase in rainfall amount for the fifth 18-year period (1992–2009) compared to the previous period 1974–1991 (Figure 7).

As the first observation in Figure 8, we can notice the big difference and the clarity of ITTA–DWT for trend identification compared to the ITA and ITTA-based original rainfall series. The trends observed in Azazga and Ain Beida (Figures 9 and 10) are similar to the Oued Taria station's partial trends. Except for new observations regarding the high rainfall, which indicates a rising trend at all of the obtained results, compared to the low and medium rainfall, especially for the Ain Beida station (Figure 9), [51] also observed,

in northeastern Algeria (Macta basin), an increasing trend in “high” rainfall. This can explain the effectiveness of ITTA–DWT for extreme event detection. The ITTA–DWT (Figures 9 and 10) indicates that region of central and eastern Algeria can face the risk the hydrological extreme in the future, explained by the torrential rainfall generating the floods, which make a natural disaster, especially in the presence of vulnerable infrastructure in the urban area. According to [91], extreme droughts in the Mediterranean Basin will not disappear progressively, but this can occur abruptly following heavy and torrential rainfall. Hence, studies on the framework of extreme rainfall events, and their impacts on the environment, are recommended for Algeria, in order to reduce the risk of flooding effects, and for sustainable development of civil engineering structures. Numerous floods were noted throughout the Algerian territory [92]: the exceptional precipitation that occurred from March 28 to 31, 1974, in several central regions, caused 52 deaths in the wilaya of Tizi–Ouzou, with 4570 houses destroyed, 130 isolated villages, and more than 18,000 disaster victims. Material damage was estimated at 27 million Dinars. Thirteen bridges and a few kilometers were washed away by the floods. Qued Rhiou in western Algeria on October 20, 1993: 22 deaths and 14 injured. Batna, Tebessa, Constantine, Ouargla, Algiers, September and October 2018: 2 deaths and material damage.

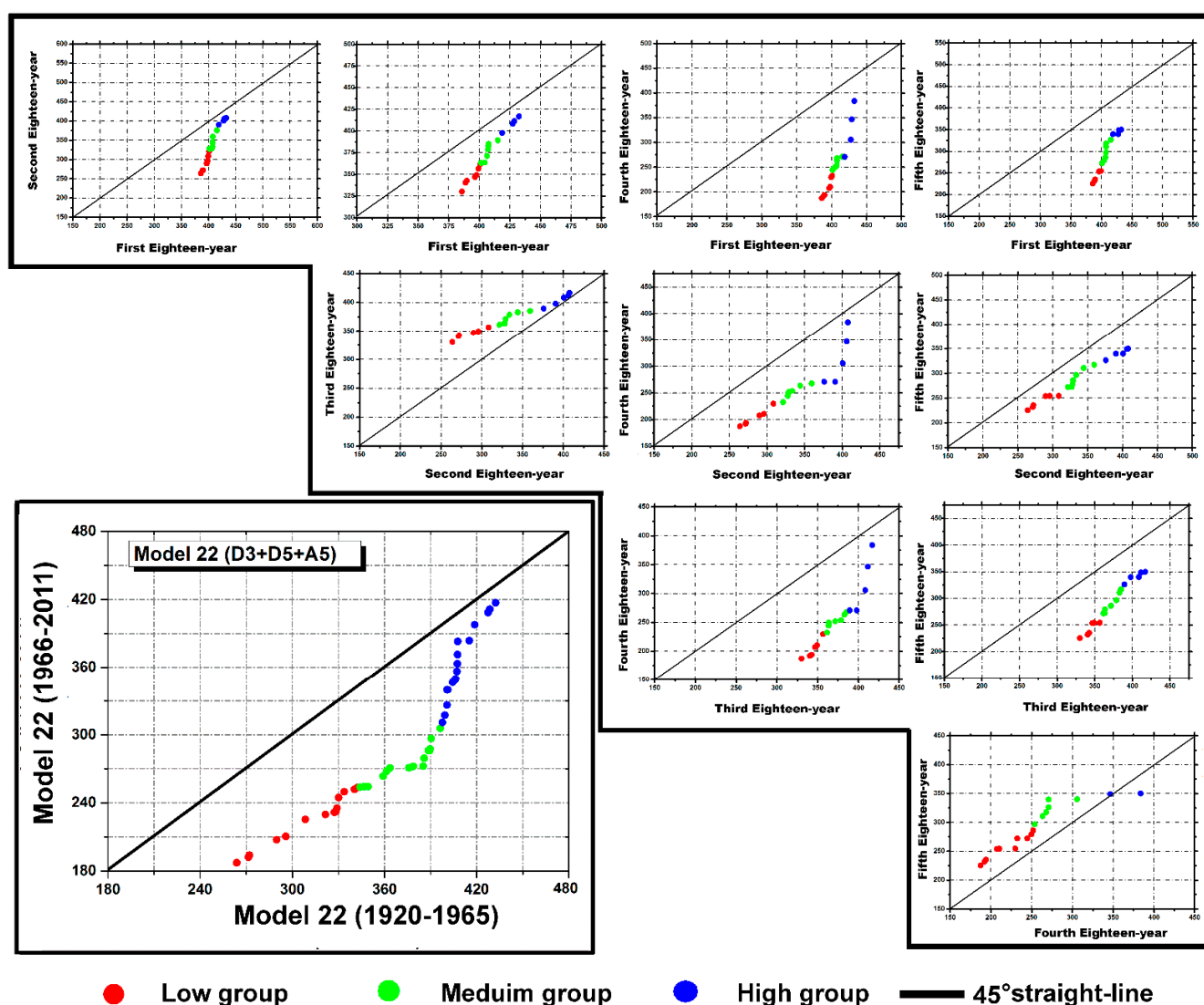


Figure 7. Triangular trend analysis methodology applied on rainfall Model (M22) resulting from DWT (ITTM–DWT: hybrid method) of Oued Taria station.

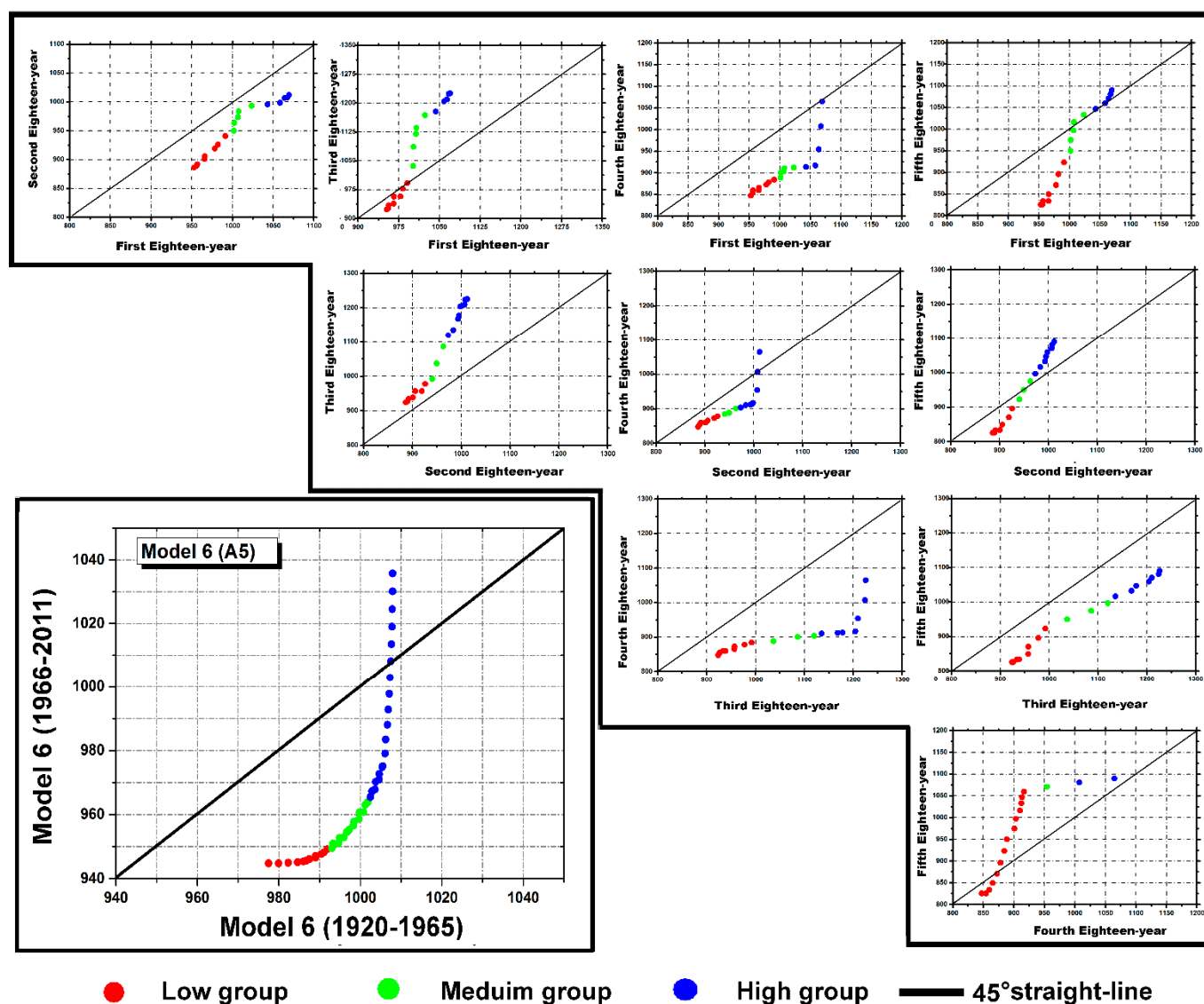


Figure 8. Triangular trend analysis methodology applied on rainfall Model (M21) resulting from DWT (ITTM–DWT: hybrid method) of Azazga station (ITM applied on model 6).

According to the analysis, the ITTA–DWT successfully detected the partial trends in the studied rainfall time series as follows:

1. A partial trend toward drier conditions occurred between 1920 and 1950.
2. A partial trend toward humid conditions occurred from 1950 to 1975.
3. A partial negative trend extended in northern Algeria from the years 1975.
4. A partial trend with a non–significant increase occurred from the end of the 1990s.

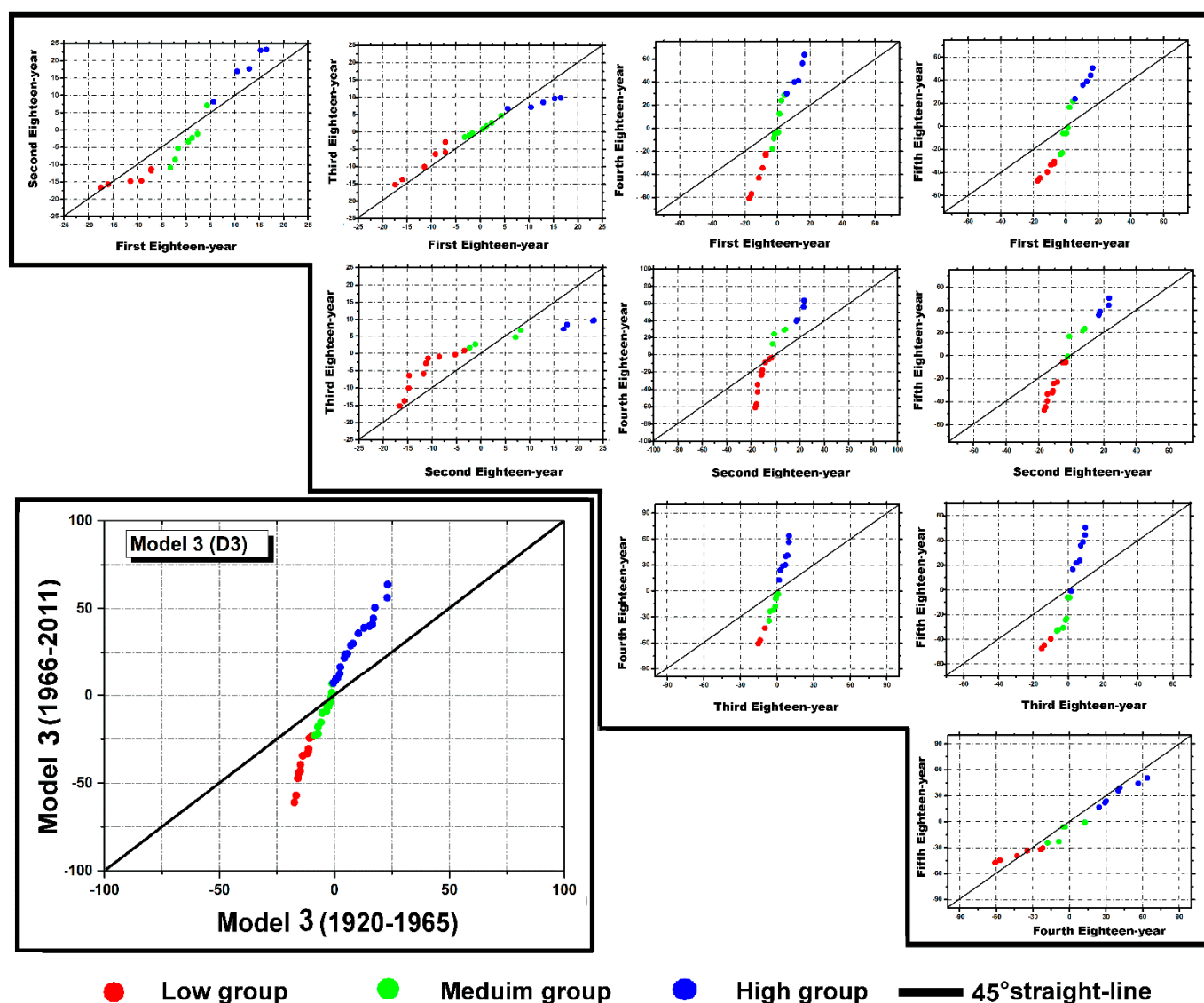


Figure 9. Triangular trend analysis methodology applied on rainfall Model (M3) resulting from DWT (ITTM–DWT: hybrid method) of Ain Beida station.

Most studies carried out in Algeria, North Africa, and the Mediterranean basin documented the existence of a negative rainfall trend and long term drought between decades 1980s and 1990s [6,12,15–17,67,68,93–102]. Over Europe and the Mediterranean basin, long-term rainfall series were analyzed by [6]; the results indicate a negative trend in the eastern Mediterranean (>2 mm/years) and approximately 0.6 mm/years in North Africa. In the northwest of Algeria at the Cheliff watershed, [12] has shown that the maximum dry episodes occurred between 1971 and 1990, where the dry sequence was negatively correlated with the Southern Oscillation phenomena explained by El Niño. In [94], the authors found, in the northern–central side of Algeria, a long-term dry period marked during the 1980s and 1990s, and it was linked to the North Atlantic Oscillation (NAO), according to a cross-analysis. In [17], researchers demonstrated—in the basins of Macta and Tafna—a wet period (upward trend) localized over the period from 1950 to 1960, accompanied by a dry period (downward trend) observed between the 1980s and 1990s. In the northwest of Algeria, [103] documented a high rainfall variability in the period 1930–2007, with a rainfall deficit extended in the region from 1975, and a wet period observed between 1930 and 1975. During the study period 1950 to 2012, [104] indicated that the most significant drought events took place in Europe, the Mediterranean region, and Baltic Republics from the 1990s

and 2000s. In Oum Er-Rabia River Basin in (Morocco), [98] observed the maximum rainfall deficit between 50 and 63% in 1980–1981 with a great spatial extent drought between the 1980s and 1990s. In [105], researchers observed that the extreme drought sequence was typical, particularly during the 1980s and 1990s. In [106], researchers observed in Chelif basin (northern Algeria) a long-wet period between 1938 and 1976, where the greatest drought episodes were observed from the year 1977. Various research concerns the slight increase in rainfall during the decade 2000–2010 compared to the 1980s–1990s, as observed in this study, but it has always been described as non-significant [92,107–109]. For example, regarding the bulk of Mediterranean areas, [110] found major downward rainfall patterns from 1901 to 2009, with no major positive patterns observed over the West Iberian Peninsula, North Africa, and Southern Italy. Likewise, [107] detected a downward trend for wet episodes in southern Italy (Basilicata region) between 1951 and 2010, where the analysis reported a non-significant positive trend during the latter decade. According to [111], detection of a rainfall pattern towards certain weather patterns can only be statistically confirmed over a dozen years.

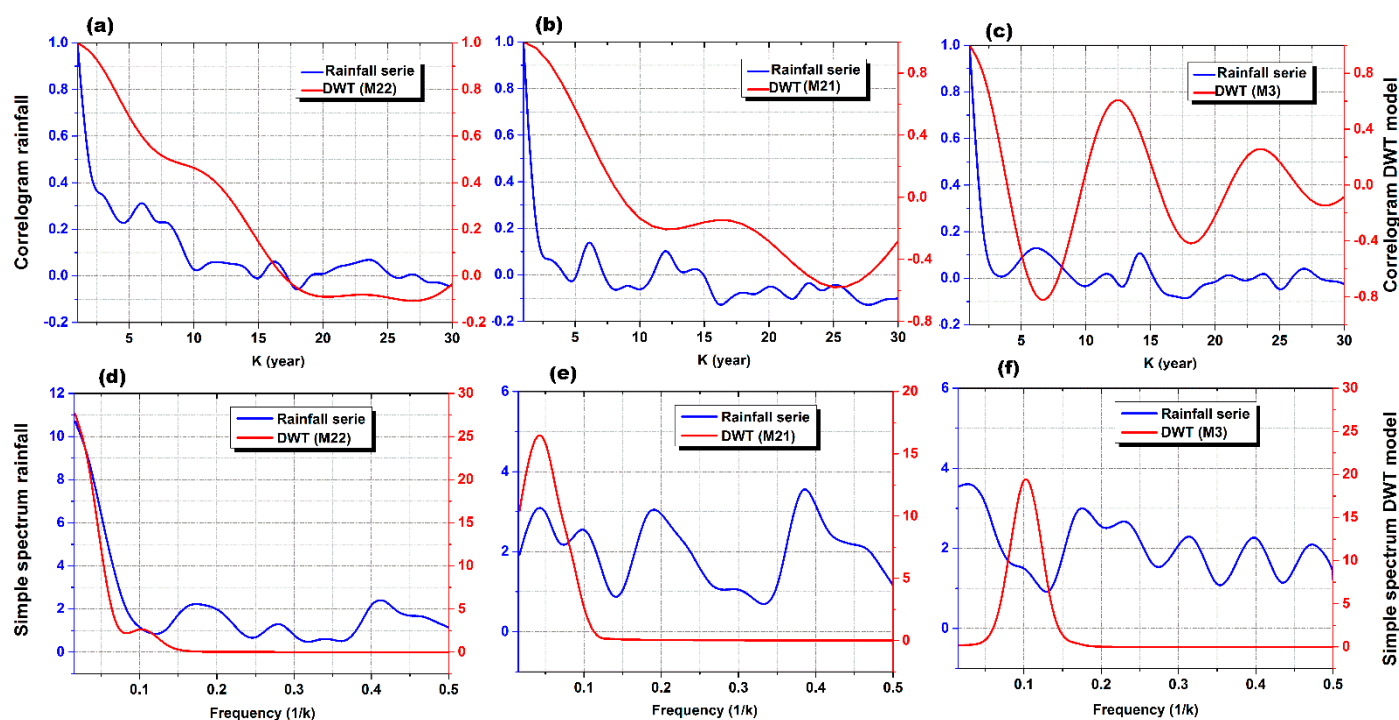


Figure 10. Correlogram of (a) Oued Taria, (b) Azazga, (c) Ain Beida rainfall (blue) and DWT model (Red) and simple spectrum of (d) Oued Taria, (e) Azazga, (f) Ain Beida rainfall (blue) and DWT model (Red).

In a previous study by [14], the correlation-spectral analysis (CSA) was applied to the original rainfall series for assessing its periodicity. In this section, CSA was also applied to the 24 combination models proposed in Table 2, to assess the cyclical components and compare them with that of the original rainfall series. Figure 10 illustrates the CSA analysis of rainfall (blue curve) and the best model of DWT (red curve) used for partial trend identification in ITTA.

The application of CSA on rainfall series indicates several fluctuations characterizing long-term organized processes explained by the dominance of inter-annual (2-years), multi-annual (5-years), and multi-decadal (20-years) rainfall periodicity fluctuations (Figure 10 blue line). The analysis of the DWT model (Figure 10 red line) indicates a spectacular peak of frequency 0.1, mainly for Azazga, describing decadal phenomena of 10 years (Figure 10d–f), unlike Oued Taria, which indicated the dominance of low-frequency phenomena of decadal and multi-decadal fluctuations, well explained by a simple spectrum (Figure 10d–f). This revealed the significant filtering process that was made based on DWT

by removing the inter-annual to multiannual fluctuations' less than decadal periodicity; for example, 90% and 61% of the energy of the original series were removed to obtain models 3 and 22, respectively (Table 1). Therefore, we can conclude from the analysis:

- The short and medium-term processes, and less than decadal periodicity, dominate the high variability of rainfall. This masks the partial trend and change points presented in the rainfall series and makes it hard to identify. In southwestern Europe, between 1850 and 2018, the authors in [21] linked the lack of substantially declining or growing patterns to the long-term rainfall series, to the predominance of inter-annual variability, making trend identification difficult. Thus, spectral analysis as a time–frequency-based method, and a first assessment tool to diagnose and characterize climatic series' high variability before inserting in trend method analyses, is indispensable.

4. Conclusions

In this paper, and based on data from representative rain gauges in northern Algeria, the partial trend identification was analyzed during 1920–2011 using ITTA and an unconventional hybrid approach (ITTA–DWT). The main results of the study are briefly outlined as follows:

- According to the analysis, the ITTA–DWT successfully detected the partial patterns in the studied rainfall time series.
- The analysis revealed the alternate long-term dry and wet periods, where most components of wet periods occurred between 1950 and 1975, with a non–significant increase in rainy episodes observed from the end of the 1990s. The dry periods were observed from 1975 to the end of the 1990s.
- The analysis indicated an increase in the occurrence of heavy rainfalls compared to low and medium intensity rainfalls, in the study area, which can infer the risk of occurrence of torrential rainfalls, which can generate floods.
- The analysis proved DWT's efficiency as a coupling method that can improve ITTA accuracy for partial trend component identification.
- The analysis proved the effectiveness of DWT as a filtering and denoising method for climatic time series.
- The inter-annual to multiannual of the short to medium processes dominate the high variability of rainfall, masking the partial trend components existing in the rainfall series, making it hard for identification.
- Before inducing the climatic time series in the trend analysis methods, the diagnosis of its behavior, and removing some components, can improve the accuracy of the analysis.
- The obtained results indicated that combining ITA, D–ITA, T–ITA, ITTA, and some input combination models resulting from the DWT is very promising, relative to those of the initial rainfall sequence. Those results corroborate the results obtained by [14]. The ITA–DWT, D–ITA–DWT, T–ITA–DWT, ITTA–DWT methods outperformed the ITA, D–ITA, T–ITA, ITTA methods for partial trend identification.

The proposed methods (ITTA–DWT) showed to be very efficient for multiscale, noise reduction, and filtering analyses; however, further studies will be needed to assess their performance using a finer time series (i.e., a monthly or daily scale) or with synthetic time series data at different variance magnitudes.

Author Contributions: B.Z. (Bilel Zerouali), M.C., N.A.-A., and M.M. conceived the framework of this research, processed data, designed the experiments, plots, and map preparation, validated the processing results, and wrote the manuscript. Z.A., C.A.G.S., B.Z. (Bilal Zerouali), A.E. gave feedback on the written manuscript, and helped to analyze and edit the manuscript for proper English language, grammar, punctuation, spelling, and technical improvements. All authors have read and agreed to the published version of the manuscript.

Funding: This research received no external funding.

Institutional Review Board Statement: Not applicable.

Informed Consent Statement: Not applicable.

Data Availability Statement: The data that support the findings of this study are owned by the National Agency of Water Resources (ANRH) of Algeria. To access and obtain the data, please contact the Agency at anrh@anrh.dz (<http://www.anrh.dz/> (accessed on 9 July 2020)).

Acknowledgments: The authors gratefully thank the Directorate General for Scientific Research and Technological Development of Algeria. We sincerely thank the three reviewers for their great constructive criticisms, valuable comments, and rich discussion. This work is dedicated to the memory of our dear best professor of the undergraduate—Urban Hydraulic section, Souk Ahras University—REZGUI Nour Eddine. You will stay the best ever.

Conflicts of Interest: The authors declare that there are no conflict of interest regarding the publication of this paper.

References

1. Verbist, K.M.J.; Maureira, H.; Rojas, P.; Vicuna, S. A stress test for climate change impacts on water security: A CRIDA case study. *Clim. Risk Manag.* **2020**, *28*, 100222. [\[CrossRef\]](#)
2. Khan, I.; Waqas, T.; Samiullah; Ullah, S. Precipitation variability and its trend detection for monitoring of drought hazard in northern mountainous region of Pakistan. *Arab. J. Geosci.* **2020**, *13*, 698. [\[CrossRef\]](#)
3. Almazroui, M.; Sen, Z.; Mohorji, A.M.; Islam, M.N. Impacts of Climate Change on Water Engineering Structures in Arid Regions: Case Studies in Turkey and Saudi Arabia. *Earth Syst. Environ.* **2018**, *3*, 43–57. [\[CrossRef\]](#)
4. Santos, C.A.G.; Brasil Neto, R.M.; da Silva, R.M.; Costa, S.G.F. Cluster analysis applied to spatiotemporal variability of monthly precipitation over Paraíba state using tropical rainfall measuring mission (TRMM) data. *Remote Sens.* **2019**, *11*, 637. [\[CrossRef\]](#)
5. Santos, C.A.; Freire, P.K.; Silva, R.M.D.; Akrami, S.A. Hybrid wavelet neural network approach for daily inflow forecasting using tropical rainfall measuring mission data. *J. Hydrol. Eng.* **2019**, *24*, 04018062. [\[CrossRef\]](#)
6. Caloiero, T.; Caloiero, P.; Frustaci, F. Long-term precipitation trend analysis in Europe and in the Mediterranean basin. *Water Environ. J.* **2018**, *32*, 433–445. [\[CrossRef\]](#)
7. Nalley, D.; Adamowski, J.; Khalil, B. Using discrete wavelet transforms to analyse trends in streamflow and precipitation in Quebec and Ontario (1954–2008). *J. Hydrol.* **2012**, *475*, 204–228. [\[CrossRef\]](#)
8. Kendall, A.; Spang, E.S. The role of industrial ecology in food and agriculture’s adaptation to climate change. *J. Ind. Ecol.* **2020**, *24*, 313–317. [\[CrossRef\]](#)
9. Xian, M.; Liu, X.; Yin, M.; Song, K.; Zhao, S.; Gao, T. Rainfall Monitoring Based on Machine Learning by Earth-Space Link in the Ku Band. *IEEE J. Sel. Top Appl. Earth Obs. Remote Sens.* **2020**, *13*, 3656–3668. [\[CrossRef\]](#)
10. Achour, K.; Meddi, M.; Zeroual, A.; Bouabdelli, S.; Maccioni, P.; Moramarco, T. Spatio-temporal analysis and forecasting of drought in the plains of northwestern Algeria using the standardized precipitation index. *J. Earth Syst. Sci.* **2020**, *129*, 42. [\[CrossRef\]](#)
11. Neama, M.A.; Attia, M.; Negm, A.; Nasr, M. Overview of Water Resources, Quality, and Management in Algeria. In *The Handbook of Environmental Chemistry*; Springer: Berlin/Heidelberg, Germany, 2020. [\[CrossRef\]](#)
12. Hallouz, F.; Meddi, M.; Mahé, G.; Rahmani, S.A.; Karahacane, H.; Brahimi, S. Analysis of meteorological drought sequences at various timescales in semi-arid climate: Case of the Cheliff watershed (northwest of Algeria). *Arab. J. Geosci.* **2020**, *13*, 280. [\[CrossRef\]](#)
13. Boudiaf, B.; Dabanli, I.; Boutaghane, H.; Şen, Z. Temperature and Precipitation Risk Assessment Under Climate Change Effect in Northeast Algeria. *Earth Syst. Environ.* **2020**, *4*, 1–14. [\[CrossRef\]](#)
14. Zerouali, B.; Chettih, M.; Abda, Z.; Mesbah, M.; Djemai, M. The use of hybrid methods for change points and trends detection in rainfall series of northern Algeria. *Acta Geophys.* **2020**, *68*, 1443–1460. [\[CrossRef\]](#)
15. Achite, M.; Buttafuoco, G.; Toubal, K.A.; Luca, F. Precipitation spatial variability and dry areas temporal stability for different elevation classes in the Macta basin (Algeria). *Environ. Earth Sci.* **2017**, *76*, 458. [\[CrossRef\]](#)
16. Taïbi, S.; Meddi, M.; Mahé, G.; Assani, A. Relationships between atmospheric circulation indices and rainfall in Northern Algeria and comparison of observed and RCM-generated rainfall. *Theor. Appl. Climatol.* **2017**, *127*, 241–257. [\[CrossRef\]](#)
17. Meddi, M.M.; Assani, A.A.; Meddi, H. Temporal Variability of Annual Rainfall in the Macta and Tafna Catchments, Northwestern Algeria. *Water Resour. Manag.* **2010**, *24*, 3817–3833. [\[CrossRef\]](#)
18. Zeroual, A.; Assani, A.A.; Meddi, M.; Alkama, R. Assessment of climate change in Algeria from 1951 to 2098 using the Köppen-Geiger climate classification scheme. *Clim. Dyn.* **2019**, *52*, 227–243. [\[CrossRef\]](#)
19. Bouabdelli, S.; Meddi, M.; Zeroual, A.; Alkama, R. Hydrological drought risk recurrence under climate change in the karst area of Northwestern Algeria. *J. Water Clim. Chang.* **2020**, jwc2020207. [\[CrossRef\]](#)
20. Öztöpal, A.; Şen, Z. Innovative Trend Methodology Applications to Precipitation Records in Turkey. *Water Resour. Manag.* **2017**, *31*, 727–737. [\[CrossRef\]](#)

21. Peña-Angulo, D.; Vicente-Serrano, S.M.; Domínguez-Castro, F.; Murphy, C.; Reig, F.; Trambly, Y.; Luna, M.Y.; Turco, M.; Noguera, I.; Aznárez-Balta, M.; et al. Long-term precipitation in Southwestern Europe reveals no clear trend attributable to anthropogenic forcing. *Environ. Res. Lett.* **2020**, *15*, 094070. [\[CrossRef\]](#)
22. Zerouali, B.; Mesbah, M.; Chettih, M.; Djemai, M.; Abda, Z. Hydrogeological System of Sebaou River Watershed (Northern Central Algeria): An Assessment of Rainfall-Runoff Relationship. In *Advances in Sustainable and Environmental Hydrology, Hydrogeology, Hydrochemistry and Water Resources*; Springer: Cham, Switzerland, 2019; pp. 29–31. [\[CrossRef\]](#)
23. Modi, A.; Tare, V.; Chaudhuri, C. Usage of long-term river discharge data in water balance model for assessment of trends in basin storages. *Model. Earth Syst. Environ.* **2020**. [\[CrossRef\]](#)
24. Singh, V.P. Hydrologic modeling: Progress and future directions. *Geosci. Lett.* **2018**, *5*, 15. [\[CrossRef\]](#)
25. Silva, R.M.; Silva, J.F.C.B.C.; Santos, C.A.G.; Brasil Neto, R.M. Spatial distribution and estimation of rainfall trends and erosivity in the Epitácio Pessoa reservoir catchment, Paraíba—Brazil. *Nat. Hazards* **2020**, *102*, 829–849. [\[CrossRef\]](#)
26. Santos, C.A.G.; Brasil Neto, R.M.; Silva, R.M.; Passos, J.S.A. Integrated spatiotemporal trends using TRMM 3B42 data for the Upper São Francisco River basin, Brazil. *Environ. Monit. Assess* **2018**, *190*, 175. [\[CrossRef\]](#) [\[PubMed\]](#)
27. Santos, C.A.G.; Kisi, O.; da Silva, R.M.; Zounemat-Kermani, M. Wavelet-based variability on streamflow at 40-year timescale in the Black Sea region of Turkey. *Arab. J. Geosci.* **2018**, *11*, 169. [\[CrossRef\]](#)
28. Atta-ur-Rahman; Dawood, M. Spatio-statistical analysis of temperature fluctuation using Mann–Kendall and Sen’s slope approach. *Clim. Dyn.* **2017**, *48*, 783–797. [\[CrossRef\]](#)
29. Rashid, M.M.; Beecham, S.; Chowdhury, R.K. Assessment of trends in point rainfall using continuous wavelet transforms. *Adv. Water Resour.* **2015**, *82*, 1–15. [\[CrossRef\]](#)
30. Da Silva, R.M.; Santos, C.A.G.; Moreira, M.; Moreira, M.; Corte-Real, J.; Silva, V.C.L.; Medeiros, I.C. Rainfall and river flow trends using Mann–Kendall and Sen’s slope estimator statistical tests in the Cobres River basin. *Nat. Hazards* **2015**, *77*, 1205–1221. [\[CrossRef\]](#)
31. Gocic, M.; Trajkovic, S. Analysis of changes in meteorological variables using Mann–Kendall and Sen’s slope estimator statistical tests in Serbia. *Glob. Planet. Chang.* **2013**, *100*, 172–182. [\[CrossRef\]](#)
32. Abungba, J.A.; Khare, D.; Pingale, S.M.; Adjei, K.A.; Gyamfi, C.; Odai, S.N. Assessment of hydro-climatic trends and variability over the black volta basin in Ghana. *Earth Syst. Environ.* **2020**, *4*, 739–755. [\[CrossRef\]](#)
33. Ajayi, V.O.; Ilori, O.W. Projected drought events over West Africa using RCA4 regional climate model. *Earth Syst. Environ.* **2020**, *4*, 329–348. [\[CrossRef\]](#)
34. Ilori, O.W.; Ajayi, V.O. Change detection and trend analysis of future temperature and rainfall over west Africa. *Earth Syst. Environ.* **2020**, *4*, 493–512. [\[CrossRef\]](#)
35. Faramarzi, N.; Sadeghnejad, S. Fluid and rock heterogeneity assessment of gas condensate reservoirs by wavelet transform of pressure-transient responses. *J. Nat. Gas Sci. Eng.* **2020**, *81*, 103469. [\[CrossRef\]](#)
36. Bolzan, M.J.A.; Franco, A.M.S.; Echer, E. A wavelet based method to remove the long term periodicities of geophysical time series. *Adv. Space Res.* **2020**, *66*, 299–306. [\[CrossRef\]](#)
37. Quilty, J.; Adamowski, J. A stochastic wavelet-based data-driven framework for forecasting uncertain multiscale hydrological and water resources processes. *Environ. Model. Softw.* **2020**, *130*, 104718. [\[CrossRef\]](#)
38. Joshi, N.; Gupta, D.; Suryavanshi, S.; Adamowski, J.; Madramootoo, C.A. analysis of trends and dominant periodicities in drought variables in India: A wavelet transform based approach. *Atmos. Res.* **2016**, *182*, 200–220. [\[CrossRef\]](#)
39. Xu, L.; Chen, N.; Zhang, X.; Chen, Z. An evaluation of statistical, NMME and hybrid models for drought prediction in China. *J. Hydrol.* **2018**, *566*, 235–249. [\[CrossRef\]](#)
40. Valipour, M. Optimization of neural networks for precipitation analysis in a humid region to detect drought and wet year alarms. *Meteorol. Appl.* **2016**, *23*, 91–100. [\[CrossRef\]](#)
41. Şen, Z. An innovative trend analysis methodology. *ASCE J. Hydrol. Eng.* **2012**, *17*, 1042–1046. [\[CrossRef\]](#)
42. Caloiero, T.; Coscarelli, R.; Ferrari, E. Assessment of seasonal and annual rainfall trend in Calabria (southern Italy) with the ITA method. *J. Hydroinform.* **2020**, *22*, 738–748. [\[CrossRef\]](#)
43. Sezen, C.; Partal, T. Wavelet combined innovative trend analysis for precipitation data in the Euphrates-Tigris basin, Turkey. *Hydrol. Sci. J.* **2020**, *65*, 1909–1927. [\[CrossRef\]](#)
44. Güçlü, Y.S. Multiple Şen-innovative trend analyses and partial Mann–Kendall test. *J. Hydrol.* **2018**, *566*, 685–704. [\[CrossRef\]](#)
45. Ali, R.; Kuriqi, A.; Abubaker, S.; Kisi, O. Long-term trends and seasonality detection of the observed flow in Yangtze River using Mann–Kendall and Sen’s innovative trend method. *Water* **2019**, *11*, 1855. [\[CrossRef\]](#)
46. Malik, A.; Kumar, A.; Guhathakurta, P.; Kisi, O. Spatial-temporal trend analysis of seasonal and annual rainfall (1966–2015) using innovative trend analysis method with significance test. *Arab. J. Geosci.* **2019**, *12*, 328. [\[CrossRef\]](#)
47. Mohorji, A.M.; Şen, Z.; Almazroui, M. Trend Analyses Revision and Global Monthly Temperature Innovative Multi-Duration Analysis. *Earth Syst. Environ.* **2017**, *1*, 9. [\[CrossRef\]](#)
48. Şen, Z. Global warming quantification by innovative trend template method. *Int. J. Global. Warm.* **2017**, *12*, 499–512. [\[CrossRef\]](#)
49. Dabanlı, İ.; Şen, Z.; Yelegen, M.Ö.; Şişman, E.; Selek, B.; Güçlü, Y.S. Trend Assessment by the Innovative-Şen Method. *Water Resour. Manag.* **2016**, *30*, 5193–5203. [\[CrossRef\]](#)
50. Tosunoglu, F.; Kisi, O. Trend analysis of maximum hydrologic drought variables using Mann–Kendall and Şen’s innovative trend method. *River Res. Appl.* **2017**, *33*, 597–610. [\[CrossRef\]](#)

51. Elouissi, A.; Şen, Z.; Habi, M. Algerian rainfall innovative trend analysis and its implications to Macta watershed. *Arab. J. Geosci.* **2016**, *9*, 303. [\[CrossRef\]](#)
52. Nourani, V.; Nezamdoost, N.; Samadi, M.; Daneshvar Vousoughi, F. Wavelet-based trend analysis of hydrological processes at different timescales. *J. Water Clim. Chang.* **2015**, *6*, 414–435. [\[CrossRef\]](#)
53. Şen, Z. Trend identification simulation and application. *J. Hydrol. Eng.* **2013**, *19*, 635–642. [\[CrossRef\]](#)
54. Şen, Z. Innovative trend significance test and applications. *Theor. Appl. Climatol.* **2017**, *127*, 939–947. [\[CrossRef\]](#)
55. Kisi, O. An innovative method for trend analysis of monthly pan evaporations. *J. Hydrol.* **2015**, *527*, 1123–1129. [\[CrossRef\]](#)
56. Alashan, S. An improved version of innovative trend analyses. *Arab. J. Geosci.* **2018**, *11*, 50. [\[CrossRef\]](#)
57. Şişman, E. Discussion of “Critical Values for Şen’s Trend Analysis” by Richard, H. McCuen. *J. Hydrol. Eng.* **2020**, *25*, 07019004. [\[CrossRef\]](#)
58. Güçlü, Y.S.; Şişman, E.; Dabanlı, İ. Innovative triangular trend analysis. *Arab. J. Geosci.* **2020**, *13*, 27. [\[CrossRef\]](#)
59. Ruggieri, E.; Antonellis, M. An exact approach to Bayesian sequential change point detection. *Comput. Stat. Data Anal.* **2016**, *97*, 71–86. [\[CrossRef\]](#)
60. Mallat, S.G. A theory for multiresolution signal decomposition: The wavelet representation. *IEEE Trans. Pattern. Anal. Mach. Intell.* **1989**, *11*, 674–693. [\[CrossRef\]](#)
61. Daubechies, I. *Ten Lectures on Wavelets*; Society for Industrial and Applied Mathematics: Philadelphia, PA, USA, 1992; p. 357. [\[CrossRef\]](#)
62. Labat, D.; Ababou, R.; Mangin, A. Analyse multirésolution croisée de pluies et débits de sources karstiques. *C. R. Geosci.* **2020**, *334*. [\[CrossRef\]](#)
63. Mangin, A. Pour une meilleure connaissance des systèmes hydrologiques à partir des analyses corrélatoire et spectrale. *J. Hydrol.* **1984**, *67*, 25–43. [\[CrossRef\]](#)
64. Amraoui, F.; Razack, M.; Bouchaou, L. Comportement d’une source karstique soumise à une sécheresse prolongée: La source Bittit (Maroc). *C. R. Geosci.* **2004**, *336*, 1099–1109. [\[CrossRef\]](#)
65. Box, G.E.; Jenkins, G.M. *Time Series Analysis: Forecasting and Control, Revised ed.*; Holden-Day: Toronto, ON, Canada, 1976.
66. Padilla, A.; Pulido-Bosch, A. Study of hydrographs of karstic aquifers by means of correlation and cross spectral analysis. *J. Hydrol.* **1995**, *168*, 73–89. [\[CrossRef\]](#)
67. Hamlaoui-Moulai, L.; Mesbah, M.; Souag-Gamane, D.; Medjerab, A. Detecting Hydro-Climatic Change Using Spatiotemporal Analysis of Rainfall Time Series in Western Algeria. *Nat. Hazards* **2013**, *65*, 1293–1311. [\[CrossRef\]](#)
68. Peña-Angulo, D.; Nadal-Romero, E.; González-Hidalgo, J.C.; Albaladejo, J.; Andreu, V.; Bagarello, V.; Barhi, H.; Batalla, R.J.; Bernal, S.; Campo, J.; et al. Spatial variability of the relationships of runoff and sediment yield with weather types throughout the Mediterranean basin. *J. Hydrol.* **2019**, *571*, 390–405. [\[CrossRef\]](#)
69. Xoplaki, E.; González-Rouco, J.F.; Luterbacher, J.; Wanner, H. Wet season Mediterranean precipitation variability: Influence of large-scale dynamics and trends. *Clim. Dynam.* **2004**, *23*, 63–78. [\[CrossRef\]](#)
70. Feki, H.; Hermassi, T.; Soualhia, N. Characterisation of mean monthly rainfall variability over mellegue catchment—Tunisia. In Proceedings of the Euro-Mediterranean Conference for Environmental Integration, Sousse, Tunisia, 20–25 November 2017; Springer: Cham, Switzerland, 2017; pp. 793–795.
71. Chargui, S.; Jaber, A.; Cudennec, C.; Lachaal, F.; Calvez, R.; Slimani, M. Statistical detection and no-detection of rainfall change trends and breaks in semiarid Tunisia—50+ years over the Merguellil agro-hydro-climatic reference basin. *Arab. J. Geosci.* **2018**, *11*, 675. [\[CrossRef\]](#)
72. Gader, K.; Gara, A.; Vanclooster, M.; Khelifi, S.; Slimani, M. Drought assessment in a south Mediterranean transboundary catchment. *Hydrol. Sci. J.* **2020**, *65*, 1300–1315. [\[CrossRef\]](#)
73. Peña-Angulo, D.; Nadal-Romero, E.; González-Hidalgo, J.C.; Albaladejo, J.; Andreu, V.; Bahri, H.; Bernal, S.; Biddoccu, M.; Bienes, R.; Campo, J.; et al. Relationship of Weather Types on the Seasonal and Spatial Variability of Rainfall, Runoff, and Sediment Yield in the Western Mediterranean Basin. *Atmosphere* **2020**, *11*, 609. [\[CrossRef\]](#)
74. Lopez-Bustins, J.A.; Lemus-Canovas, M. The influence of the Western Mediterranean Oscillation upon the spatio-temporal variability of precipitation over Catalonia (northeastern of the Iberian Peninsula). *Atmos. Res.* **2020**, *236*, 104819. [\[CrossRef\]](#)
75. Ellouze, M.; Azri, C.; Abida, H. Spatial variability of monthly and annual rainfall data over Southern Tunisia. *Atmos. Res.* **2009**, *93*, 832–839. [\[CrossRef\]](#)
76. Vaseghi, S.V. *Advanced Digital Signal Processing and Noise Reduction*; John Wiley & Sons: Hoboken, NJ, USA, 2008.
77. Kim, S.; Noh, H.; Kang, N.; Lee, K.; Kim, Y.; Lim, S.; Lee, D.R.; Kim, H.S. Noise reduction analysis of radar rainfall using chaotic dynamics and filtering techniques. *Adv. Meteorol.* **2014**, *2014*, 517571. [\[CrossRef\]](#)
78. Jayawardena, A.W.; Gurung, A.B. *Effect of Noise in Nonlinear Hydrological Time Series Analysis and Prediction*; No. 255; International Association of Hydrological Sciences Publication: Wallingford, UK, 1999; pp. 121–128.
79. Adamowski, K.; Prokoph, A.; Adamowski, J. Development of a new method of wavelet aided trend detection and estimation. *Hydrol. Process.* **2009**, *23*, 2686–2696. [\[CrossRef\]](#)
80. Palizdan, N.; Falamarzi, Y.; Huang, Y.F.; Lee, T.S. Precipitation trend analysis using discrete wavelet transform at the Langat River Basin, Selangor, Malaysia. *Stoch. Environ. Res. Risk A* **2017**, *31*, 853–877. [\[CrossRef\]](#)
81. Pandey, B.; Tiwari, H.; Khare, D. Trend analysis using discrete wavelet transform (DWT) for long-term precipitation (1851–2006) over India. *Hydrolog. Sci. J.* **2017**, *62*, 2187–2208. [\[CrossRef\]](#)

82. Pathak, P.; Kalra, A.; Ahmad, S.; Bernardez, M. Wavelet-aided analysis to estimate seasonal variability and dominant periodicities in temperature, precipitation, and streamflow in the Midwestern United States. *Water Resour. Manag.* **2016**, *30*, 4649–4665. [\[CrossRef\]](#)
83. Partal, T. Multi-annual analysis and trends of the temperatures and precipitations in West Anatolia. *J. Water Clim. Chang.* **2017**, jwc2017109. [\[CrossRef\]](#)
84. Sang, Y.F.; Sun, F.; Singh, V.P.; Xie, P.; Sun, J. A discrete wavelet spectrum approach for identifying non-monotonic trends in hydroclimate data. *Hydrol. Earth Syst. Sci.* **2018**, *22*, 757–766. [\[CrossRef\]](#)
85. Freire, P.K.D.M.M.; Santos, C.A.G.; da Silva, G.B.L. Analysis of the use of discrete wavelet transforms coupled with ANN for short-term streamflow forecasting. *Appl. Soft. Comput.* **2019**, *80*, 494–505. [\[CrossRef\]](#)
86. Abda, Z.; Chettih, M.; Zerouali, B. Assessment of neuro-fuzzy approach based different wavelet families for daily flow rates forecasting. *Model. Earth Syst. Environ.* **2020**. [\[CrossRef\]](#)
87. Kisi, O.; Alizamir, M.; Shiri, J. Conjunction Model Design for Intermittent Streamflow Forecasts: Extreme Learning Machine with Discrete Wavelet Transform. In *Intelligent Data Analytics for Decision-Support Systems in Hazard Mitigation*; Springer: Singapore, 2020; pp. 171–181. [\[CrossRef\]](#)
88. Pal, L.; Ojha, C.S.P.; Chandniha, S.K.; Kumar, A. Regional scale analysis of trends in rainfall using nonparametric methods and wavelet transforms over a semi-arid region in India. *Int. J. Climatol.* **2019**, *39*, 2737–2764. [\[CrossRef\]](#)
89. Adarsh, S.; Janga Reddy, M. Trend analysis of rainfall in four meteorological subdivisions of southern India using nonparametric methods and discrete wavelet transforms. *Int. J. Climatol.* **2015**, *35*, 1107–1124. [\[CrossRef\]](#)
90. Araghi, A.; Baygi, M.M.; Adamowski, J.; Malard, J.; Nalley, D.; Hasheminia, S.M. Using wavelet transforms to estimate surface temperature trends and dominant periodicities in Iran based on gridded reanalysis data. *Atmos. Res.* **2015**, *155*, 52–72. [\[CrossRef\]](#)
91. Gómez Navarro, L. *Aproximación Metodológica al Estudio de Secuencias Secas de Larga Duración: El Caso de las Islas Baleares*; Publicaciones de la Asociación Española de Climatología: Zaragoza, Spain, 2002.
92. Khoulalia, W.; Djebbar, Y.; Hammar, Y. Caractérisation de la variabilité climatique: Cas du bassin versant de la Medjerda (Nord-Est algérien). *Synthèse Revue Sci. Technol.* **2014**, *29*, 6–23.
93. Khedimallah, A.; Meddi, M.; Mahé, G. Characterization of the interannual variability of precipitation and runoff in the Cheliff and Medjerda basins (Algeria). *J. Earth Syst. Sci.* **2020**, *129*, 134. [\[CrossRef\]](#)
94. Zerouali, B.; Mesbah, M.; Chettih, M.; Djemai, M. Contribution of cross time-frequency analysis in assessment of possible relationships between large-scale climatic fluctuations and rainfall of northern central Algeria. *Arab. J. Geosci.* **2018**, *11*, 392. [\[CrossRef\]](#)
95. Elmeddahi, Y.; Issaadi, A.; Mahmoudi, H.; Tahar Abbes, M.; Goosen Mattheus, F.A. Effect of climate change on water resources of the Algerian Middle Cheliff basin. *Desalination Water Treat.* **2014**, *52*, 2073–2081. [\[CrossRef\]](#)
96. Mrad, D.; Dairi, S.; Boukhari, S.; Djebbar, Y. Applied multivariate analysis on annual rainfall in the northeast of Algeria. *J. Water Clim. Chang.* **2019**. [\[CrossRef\]](#)
97. Sangüesa-Barreda, G.; Camarero, J.J.; Sánchez-Salguero, R.; Gutiérrez, E.; Linares, J.C.; Génova, M.; Ribas, M.; Tiscar, P.A.; López-Sáez, J.A. Droughts and climate warming desynchronize Black pine growth across the Mediterranean Basin. *Sci. Total Environ.* **2019**, *697*, 133989. [\[CrossRef\]](#) [\[PubMed\]](#)
98. Ouati, H.; Boudhar, A.; Ouhinou, A.; Arioua, A.; Hssaisoune, M.; Bouamri, H.; Benabdelouahab, T. Trend analysis of rainfall and drought over the Oum Er-Rbia River Basin in Morocco during 1970–2010. *Arab. J. Geosci.* **2019**, *12*, 128. [\[CrossRef\]](#)
99. Spinoni, J.; Vogt, J.V.; Naumann, G.; Barbosa, P.; Dosio, A. Will drought events become more frequent and severe in Europe? *Int. J. Climatol.* **2018**, *38*, 1718–1736. [\[CrossRef\]](#)
100. Coll, J.R.; Aguilar, E.; Ashcroft, L. Drought variability and change across the Iberian Peninsula. *Theor. Appl. Climatol.* **2017**, *130*, 901–916. [\[CrossRef\]](#)
101. Achite, M.; Ouillon, S. Recent changes in climate, hydrology and sediment load in the Wadi Abd, Algeria (1970–2010). *Hydrol. Earth Syst. Sci.* **2016**, *20*, 1355–1372. [\[CrossRef\]](#)
102. Jemai, H.; Ellouze, M.; Abida, H.; Laignel, B. Spatial and temporal variability of rainfall: Case of Bizerte-Ichkeul Basin (Northern Tunisia). *Arab. J. Geosci.* **2018**, *11*, 177. [\[CrossRef\]](#)
103. Meddi, H.; Meddi, M.; Assani, A.A. Study of Drought in Seven Algerian Plains. *Arab. J. Sci. Eng.* **2014**, *39*, 339–359. [\[CrossRef\]](#)
104. Spinoni, J.; Naumann, G.; Vogt, J.V.; Barbosa, P. The biggest drought events in Europe from 1950 to 2012. *J. Hydrol. Reg. Stud.* **2015**, *3*, 509–524. [\[CrossRef\]](#)
105. Ruiz Sinoga, J.D.; León Gross, T. Droughts and their social perception in the mass media (southern Spain). *Int. J. Climatol.* **2013**, *33*, 709–724. [\[CrossRef\]](#)
106. Derdous, O.; Bouamrane, A.; Mrad, D. Spatiotemporal analysis of meteorological drought in a Mediterranean dry land: Case of the Cheliff basin–Algeria. *Model. Earth Syst. Environ.* **2020**. [\[CrossRef\]](#)
107. Piccarreta, M.; Pasini, A.; Capolongo, D.; Lazzari, M. Changes in Daily Precipitation Extremes in the Mediterranean from 1951 to 2010: The Basilicata Region, Southern Italy. *Int. J. Climatol.* **2013**, *33*, 3229–3248. [\[CrossRef\]](#)
108. Khezazna, A.; Amarchi, H.; Derdous, O.; Bousakhria, F. Drought monitoring in the Seybouse basin (Algeria) over the last decades. *Water Land. Dev.* **2017**, *33*, 79–88. [\[CrossRef\]](#)
109. Zeineddine, N.; Ovidiu, M. Rainfall Variability and Trend Analysis of Annual Rainfall in North Africa. *Int. J. Earth Atmos. Sci.* **2016**, *2016*, 7230450. [\[CrossRef\]](#)

-
110. Philandras, C.M.; Nastos, P.T.; Kapsomenakis, J.; Douvis, K.C.; Tselioudis, G.; Zerefos, C.S. Long term precipitation trends and variability within the Mediterranean region. *Nat. Hazard Earth Sys.* **2011**, *11*, 3235–3250. [[CrossRef](#)]
 111. Ozer, P.; Erpicum, M.; Demarée, G.; Vandiepenbeeck, M. The Sahelian drought may have ended during the 1990s. *Hydrolog. Sci. J.* **2003**, *48*, 489–492. [[CrossRef](#)]